J. Fluid Mech. (1999), *vol.* 381, *pp.* 63–87. Printed in the United Kingdom

The inertial lift on a spherical particle in a plane Poiseuille flow at large channel Reynolds number

By EVGENY S. ASMOLOV

Zhukovsky Central Aero-Hydrodynamics Institute, Zhukovsky, Moscow Region, 140160, Russia
e-mail: aes@an.aerocentr.msk.su

(Received 28 February 1997 and in revised form 10 September 1998)

The inertial migration of a small rigid sphere translating parallel to the walls within a channel flow at large channel Reynolds numbers is investigated. The method of matched asymptotic expansions is used to solve the equations governing the disturbance flow past a particle at small particle Reynolds number and to evaluate the lift. Both neutrally and non-neutrally buoyant particles are considered. The wall-induced inertia is significant in the thin layers near the walls where the lift is close to that calculated for linear shear flow, bounded by a single wall. In the major portion of the flow, excluding near-wall layers, the wall effect can be neglected, and the outer flow past a sphere can be treated as unbounded parabolic shear flow. The effect of the curvature of the unperturbed velocity profile is significant, and the lift differs from the values corresponding to a linear shear flow even at large Reynolds numbers.

1. Introduction

A rigid spherical particle translating at small Reynolds number in a shear flow field experiences a lift. No lateral force can be deduced on the basis of creeping-flow equations whatever the undisturbed velocity profile (Bretherton 1962). Hence it is due to the small inertia and wall effect. It results in particle migration across the streamlines of an undisturbed, laminar flow. Such a motion was first observed by Segré & Silberberg (1962 *a*, *b*) for dilute suspension flow through a pipe. The Reynolds number based on the pipe width was in the interval from 2 to 700. It was found that the concentration distribution of neutrally buoyant particles is non-uniform with maximum concentration being at radial position 0.6 of a pipe radius from the centreline. Experiments on inertial migration of non-neutrally buoyant particles within a vertical channel flow were performed by Jeffrey & Pearson (1965) and Eichorn & Small (1964). They showed that a particle migrates towards the channel walls when it leads the undisturbed flow, whereas for the case when its velocity is less, migration in the opposite direction takes place. Vasseur & Cox (1977) measured the migration velocity of a small sphere sedimenting in a stagnant fluid bounded by a flat vertical wall. In this case a sphere always migrates away from the wall. Cherukat, McLaughlin & Graham (1994) investigated inertial migration in a linear shear flow between two vertical walls.

Theoretical studies of the inertia effect were based on the solution of Navier–Stokes equations using perturbation methods. At small particle Reynolds number the disturbance flow to leading order is governed by creeping-flow equations. Even though the inertial terms are small compared with viscous ones at distances of the

order of the particle radius, a, from particle centre (inner region), they are of the same order at sufficiently large distance from the sphere (outer region).

The regular perturbation technique can be used when the distance of the particle from the wall is small compared with the lengthscale of the outer region, i.e. it is assumed that the wall lies within the inner region of the flow. Cox & Brenner (1968) considered the migration of a non-neutrally buoyant sphere translating in a linear shear flow near a flat wall. They expressed the lift in terms of Green's functions. Ho & Leal (1974) studied the migration of a neutrally buoyant sphere in a planar flow bounded by two flat walls. Vasseur & Cox (1976) and Cox & Hsu (1977) employed the regular perturbation technique to evaluate the lift in a linear and parabolic wall-bounded flow.

When the flow is unbounded or the walls lie in the outer region the method of matched asymptotic expansions is used to solve the Oseen-like equations governing the disturbance flow and to calculate the lift. Saffman (1965) studied the inertial migration of a small sphere in an unbounded linear shear flow for the strong shear limit when the two particle Reynolds numbers, based on the slip velocity, V', and the shear rate, G, respectively,

$$R_V = a|V'|/\nu \ll 1, \qquad R_G = Ga^2/\nu \ll 1, \tag{1.1}$$

are assumed to satisfy $R_V \ll R_G^{1/2}$. In this case the uniform flow in the undisturbed velocity profile can be neglected. Saffman showed that to the leading order the lift can be obtained by approximating the sphere by a point force in the outer region. One need only compute the transverse component of the velocity at the particle centre and use the Stokes drag law to calculate the lift. The effect of a distant wall for the strong shear limit was considered by Drew (1988) and Asmolov (1989).

The opposite, weak-shear limiting case, $R_V \gg R_G^{1/2}$, was considered by Vasseur & Cox (1977). They calculated the migration velocity of a particle sedimenting in stagnant fluid bounded by one or two plane walls.

Asmolov (1990) and McLaughlin (1991, 1993) independently calculated the lift on a particle moving in a linear shear flow (unbounded or bounded by a single planar wall). They removed Saffman's restriction on the ratio $\alpha = R_V/R_G^{1/2}$, characterizing the relative size of the uniform and linear terms in the undisturbed velocity profile.

The migration within the channel flow for Reynolds number $R_c = U'_m l/\nu$ of less than approximately 100 was investigated for neutrally buoyant (Schonberg & Hinch 1989) and non-neutrally buoyant (Hogg 1994) particles. Here U'_m is the maximum velocity of a channel flow, l is the channel width. The studies of Schonberg & Hinch (1989) and Hogg (1994) demonstrate that to leading order the effects of the uniform flow and the shear may be combined in the governing equations of the outer flow.

Hogg investigated the strong and weak shear limits for a non-neutrally buoyant sphere. He does not systematically expound the general case, $\alpha = O(1)$, but calculated the variation of the equilibrium position at $R_c = 1$ for a range of values of α, including $\alpha = O(1)$.

The main object of the present paper is to calculate the lift on a small sphere in a channel flow for large R_c. The particle Reynolds numbers R_V and R_G are taken to be the asymptotically small parameters while the channel Reynolds number is finite. It is assumed that $\alpha = O(1)$ but there is no relationship between R_V and R_c, so that R_c remains the same as R_V tends to zero. Cases of both a non-neutrally buoyant particle translating parallel to the walls with arbitrary α and a neutrally buoyant particle are

considered. The study fills the gap between the results obtained for a linear shear flow and channel flow.

The lengthscale of the outer region for the two flows are defined in different ways. For a linear shear flow the lengthscale based on the local value of the shear rate at the sphere centre, G,

$$l_G = aR_G^{-1/2} = \left(\nu/G\right)^{1/2}, \tag{1.2}$$

was used (Saffman 1965; Drew 1988; Asmolov 1989, 1990; McLaughlin 1991, 1993). For the problem in question $G = \gamma U'_m/l$, where $\gamma = 4 - 8d/l$ is the dimensionless shear rate at the particle centre, d is the distance between the particle centre and the nearest wall.

For a sphere translating in a channel flow the particle Reynolds number and the lengthscale of the outer region based on the average shear rate, U'_m/l, was introduced (Schonberg & Hinch 1989; Hogg 1994):

$$R_p = U'_m a^2/\nu l, \qquad l_p = aR_p^{-1/2} = \left(\nu l/U'_m\right)^{1/2} = lR_c^{-1/2}. \tag{1.3}$$

Two Reynolds numbers and lengthscales introduced by (1.1), (1.2) and (1.3) are related as

$$R_G = \gamma R_p, \qquad l_G = \left[\frac{\nu l}{\gamma U'_m}\right]^{1/2} = l\left(\gamma R_c\right)^{-1/2} = l_p\gamma^{-1/2}.$$

The ratios of the lengthscales l_p, l_G, to l decrease with R_c and for large channel Reynolds number are small compared with the channel width.

For the problem in question approaches using either l_p or l_G as a lengthscale of the outer region have some advantages and disadvantages. Since R_p, l_p do not depend on particle position the approach based on definitions (1.3) is more convenient to compare the results calculated for given R_c and slip velocity and various particle positions.

On the other hand, the outer region around the particle at large R_c is only a small portion of the flow, and the lift will depend on the local shear rate rather than its average value. In order to correlate the results of calculations of the lift in a channel flow with linear-shear predictions it is useful to scale the disturbance flow in terms of R_G, l_G. The curvature of the undisturbed velocity scaled by l_G tends to zero as $R_c \to \infty$, except very near the centre of the channel, where $\gamma \sim 8/R_c$. Hence the effects of both the curvature and of the second far-removed wall (or both walls when d is large compared with $lR_c^{-1/2}$) become small at large channel Reynolds numbers. As a result one would expect that the lift tends to the value appropriate to the linear shear flow bounded by a single wall (or to unbounded flow). However, this approach is inapplicable when the particle is near the centreline of the channel, since we have $G = 0$ and $l_G \to \infty$ on the centreline.

We present analyses for both approaches. The dimensionless equations and boundary conditions for a small rigid sphere translating parallel to the walls are derived in § 2. In § 3, the inner solution valid at a distance comparable with the sphere radius is constructed for a non-neutrally buoyant particle. Following the approach of Hogg (1994) the analysis of the outer problem based on the l_p lengthscale is developed. The ordinary differential equation for the Fourier transform of the lateral velocity is solved numerically using the orthonormalization method.

In § 4, the solution of the outer problem based on the l_G lengthscale is obtained. This approach makes it possible to classify more clearly the effects due to the inertia

in the unbounded flow and the inertial interaction with the walls. The wall effect is significant in the thin layers, at distances of the order of $lR_c^{-1/2}$ from the walls, where the lift is close to the values appropriate to the linear shear flow bounded by a single wall. For the major portion of the channel, excluding these layers, the wall effect can be neglected, and the disturbance flow can be treated as unbounded. However, the effect of the curvature of the undisturbed velocity is still sizeable in this part of the flow even at large channel Reynolds number, and lift depends on two dimensionless groups characterizing the relative sizes of the uniform, linear and parabolic terms in the undisturbed velocity profile.

The flow disturbance past a neutrally buoyant particle is due to the shear on the sphere. This case is considered in §§ 5 and 6 on the basis of the l_p and l_G scaling, respectively, of the outer-flow equations. The wall effect again emerges in the thin layers near the walls. In the remainder of the channel flow, where the wall-induced inertia is negligible, the lift is significantly less. For the unbounded case it depends on the curvature of the undisturbed velocity only. The lift is also evaluated for a neutrally buoyant sphere in a linear shear flow bounded by a single wall.

The comparison with the experimental results is made in § 7. Finally, the results are summarized in § 8.

2. Governing equations

Consider a rigid sphere of radius a moving parallel to the walls within a plane Poiseuille flow (figure 1). The origin of the coordinate system is at the centre of the sphere and translates with the particle velocity $\boldsymbol{U}'_p = U'_p \boldsymbol{e}_x$ where $\boldsymbol{e}_x$ is a unit vector aligned with the x-axis. The particle is at rest in this frame of reference, while the walls translate with constant velocity. Thus, the flow considered is steady. The particle slip velocity, introduced by $V' = 4U'_m d\,(l-d)\,/l^2 - U'_p$, is taken to be non-zero in general. The undisturbed flow is

$$\bar{\boldsymbol{v}}' = \left[V' + U'_m\left(\gamma\frac{z'}{l} - 4\frac{z'^2}{l^2}\right)\right]\boldsymbol{e}_x. \tag{2.1}$$

Hereinafter a prime is used to denote dimensional velocities and space coordinates. The equations and boundary conditions governing the disturbance flow (the flow being the difference between the actual flow and that given by (2.1)) are (Hogg 1994)

$$\boldsymbol{u}'\cdot\nabla'\boldsymbol{u}' + \bar{\boldsymbol{v}}'\cdot\nabla'\boldsymbol{u}' + \boldsymbol{u}'\cdot\nabla'\bar{\boldsymbol{v}}' = -\nabla' p'/\rho + \nu\nabla'^2\boldsymbol{u}', \tag{2.2a}$$

$$\nabla'\cdot\boldsymbol{u}' = 0, \tag{2.2b}$$

$$\boldsymbol{u}' = \boldsymbol{\Omega}'_p \wedge \boldsymbol{r}' - \bar{\boldsymbol{v}}' \quad \text{on} \quad r' = a, \tag{2.2c}$$

$$\boldsymbol{u}' = 0 \quad \text{on} \quad z' = -d,\ l-d, \tag{2.2d}$$

$$\boldsymbol{u}' \to 0 \quad \text{as} \quad x' \to \infty, \tag{2.2e}$$

where $\boldsymbol{r}' = (x', y', z')$, $r' = |\boldsymbol{r}'|$, and $\boldsymbol{\Omega}'_p$ is the rotational velocity of the sphere.

Dimensionless variables are introduced by

$$\boldsymbol{r} = \boldsymbol{r}'/a, \quad \boldsymbol{u} = \boldsymbol{u}'/U'_m, \quad \boldsymbol{\Omega}_p = \boldsymbol{\Omega}'_p l/U'_m, \quad \boldsymbol{F} = \boldsymbol{F}'/\mu a U'_m,$$

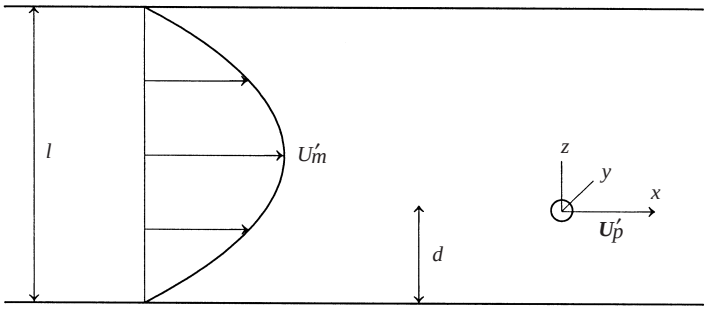

FIGURE 1. Configuration of the flow and the coordinate system.

where $\boldsymbol{F}$ is a dimensionless force on a sphere. The basic asymptotic parameter in the problem is defined as $\epsilon = R_p^{1/2}$. All other dimensionless groups are taken to be of the order of unity or can be expressed in terms of some power of ϵ. So it is assumed that $V = V'/U'_m = O(1)$, $d/l = O(1)$. It should be stressed that even though we consider large channel Reynolds numbers, R_c remains the same as R_p tends to zero. For the ratio of particle size to channel width taking account of (1.3) we have $a/l = \left(R_p/R_c\right)^{1/2} = \epsilon R_c^{-1/2}$. The dimensionless undisturbed velocity field can be written as

$$\bar{\boldsymbol{v}} = \bar{\boldsymbol{v}}'/U'_m = \left(V + \epsilon\gamma z R_c^{-1/2} - 4\epsilon^2 z^2 R_c^{-1}\right)\boldsymbol{e}_x. \tag{2.3}$$

Then equations (2.2) are rewritten in dimensionless form as

$$\epsilon R_c^{1/2}\left(\boldsymbol{u}\cdot\nabla\boldsymbol{u} + \bar{\boldsymbol{v}}\cdot\nabla\boldsymbol{u} + \boldsymbol{u}\cdot\nabla\bar{\boldsymbol{v}}\right) = -\nabla p + \nabla^2\boldsymbol{u}, \tag{2.4a}$$

$$\nabla\cdot\boldsymbol{u} = 0, \tag{2.4b}$$

$$\boldsymbol{u} = -V\boldsymbol{e}_x + \epsilon R_c^{-1/2}\left(\boldsymbol{\Omega}_p\wedge\boldsymbol{r} - \gamma z\boldsymbol{e}_x\right) + 4\epsilon^2 z^2 R_c^{-1}\boldsymbol{e}_x \quad \text{on} \quad r = 1, \tag{2.4c}$$

$$\boldsymbol{u} = 0 \quad \text{on} \quad z = -\epsilon^{-1}R_c^{1/2}d/l, \quad \epsilon^{-1}R_c^{1/2}\left(1 - d/l\right), \tag{2.4d}$$

$$\boldsymbol{u}\to 0 \quad \text{as} \quad x\to\infty. \tag{2.4e}$$

For a non-neutrally buoyant spherical particle falling in a vertical channel $V = O(1)$. It is seen from (2.4 *c*) that the disturbance flow is also of the order of unity. The disturbance is due to the shear on the sphere and particle rotation when $|V| \ll \epsilon^2/R_c$. It follows from (2.4 *c*) that $\boldsymbol{u}$, $p = O(\epsilon)$ in this case.

3. Non-neutrally buoyant particle

Much of §§ 3.1, 3.2 follows Schonberg & Hinch (1989) and Hogg (1994). The velocity and pressure fields and the force on a sphere for the case when $V = O(1)$ are sought in the form

$$\boldsymbol{u} = \boldsymbol{u}_0 + \epsilon\boldsymbol{u}_1 + o(\epsilon), \qquad p = p_0 + \epsilon p_1 + o(\epsilon), \qquad \boldsymbol{F} = \boldsymbol{F}_0 + \epsilon\boldsymbol{F}_1 + o(\epsilon). \tag{3.1}$$

3.1. *The inner solution*

The equations for $\boldsymbol{u}_0$, p_0 can be derived by substituting (3.1) into (2.4) and collecting the terms of power ϵ^0. Then the main-order governing equations reduce to creeping-

flow equations in an unbounded fluid, and one can write

$$\nabla^2 \boldsymbol{u}_0 - \nabla p_0 = 0, \tag{3.2a}$$

$$\nabla \cdot \boldsymbol{u}_0 = 0, \tag{3.2b}$$

$$\boldsymbol{u}_0 = -V\boldsymbol{e}_x \quad \text{on} \quad r = 1, \tag{3.2c}$$

$$\boldsymbol{u}_0 \to 0 \quad \text{as} \quad r \to \infty. \tag{3.2d}$$

It should be noted that boundary condition (3.2 *c*), in contrast to that in Hogg (1994), contains only the slip velocity. The terms corresponding to the shear rate and particle angular velocity are of the order of ϵ, and that corresponding to the curvature of the velocity profile is of order ϵ^2. Hence they should be omitted for the main-order problem. Solution of (3.2) is

$$\boldsymbol{u}_0 = -V\left[\boldsymbol{e}_x\left(\frac{3}{4r} + \frac{1}{4r^3}\right) + \frac{3}{4}\frac{x\boldsymbol{r}}{r^2}\left(\frac{1}{r} - \frac{1}{r^3}\right)\right]. \tag{3.3}$$

This axisymmetric solution gives the drag on the sphere, $\boldsymbol{F}_0 = 6\pi V\boldsymbol{e}_x$ and no lateral force or torque. The lift comes from the second term in the inner solution, so that $F_z = \epsilon F_{1z}$. Collecting the terms of like power of ϵ in the expansion of equations (2.4) one can derive, taking account of (2.3), the equations for $\boldsymbol{u}_1$, p_1:

$$\nabla^2 \boldsymbol{u}_1 - \nabla p_1 = R_c^{1/2}(\boldsymbol{u}_0 + V\boldsymbol{e}_x)\cdot\nabla\boldsymbol{u}_0, \tag{3.4a}$$

$$\nabla \cdot \boldsymbol{u}_1 = 0, \tag{3.4b}$$

$$\boldsymbol{u}_1 = R_c^{-1/2}\left(\boldsymbol{\Omega}_p \wedge \boldsymbol{r} - \gamma z\boldsymbol{e}_x\right) \quad \text{on} \quad r = 1. \tag{3.4c}$$

Note that even to this order the curvature of the velocity profile does not enter into the inner-flow equations. $\boldsymbol{u}_1$ does not decay at infinity, and the boundary condition at infinity has to be replaced by a matching condition with the outer flow.

The equations (3.4) are linear, and the velocity field can be sought in the following form:

$$\boldsymbol{u}_1 = \boldsymbol{u}_0^{nb} + R_c^{1/2}\boldsymbol{u}_1^{PP} + \boldsymbol{V}_1. \tag{3.5}$$

Here $\boldsymbol{u}_0^{nb}$ is the solution of the homogeneous part of (3.4 *a*), i.e. of the creeping-flow equations, satisfying the boundary condition (3.4 *c*), $R_c^{1/2}\boldsymbol{u}_1^{PP}$ is the solution of (3.4 *a*) with $\boldsymbol{u}_1 = 0$ on $r = 1$, and $\boldsymbol{V}_1$ is a solution of the creeping-flow equations that matches a uniform flow at infinity and satisfies $\boldsymbol{V}_1 = 0$ on $r = 1$.

$\boldsymbol{u}_0^{nb}$ is the same as the main-order solution for a neutrally buoyant particle and is given by (5.3). For $\boldsymbol{u}_1^{PP}$ we have (Proudman & Pearson 1957)

$$\boldsymbol{u}_1^{PP} = \frac{3}{32}V^2\left[\left(2 - \frac{3}{r} + \frac{1}{r^2} - \frac{1}{r^3} + \frac{1}{r^4}\right)\left(1 - \frac{3x^2}{r^2}\right)\frac{\boldsymbol{r}}{r} + \left(4 - \frac{3}{r} + \frac{1}{r^3} - \frac{2}{r^4}\right)\left(\frac{x^2\boldsymbol{r}}{r^3} - \frac{x\boldsymbol{e}_x}{r}\right)\right].$$

Because of the symmetry the regular perturbation expansion (the terms $\boldsymbol{u}_0^{nb}$ and $R_c^{1/2}\boldsymbol{u}_1^{PP}$) gives no lift force on a sphere. It comes only from $\boldsymbol{V}_1$, which is found from the matching condition.

The outer spatial coordinates are introduced by the scaling $\boldsymbol{R} = (X, Y, Z) = \epsilon \boldsymbol{r}$. When written in outer variables (3.3) gives

$$\boldsymbol{u}_0 = \epsilon \boldsymbol{U}_s + O\left(\epsilon^3\right),$$

where

$$\boldsymbol{U}_s = -\frac{3}{4} V \left(\frac{\boldsymbol{e}_x}{R} + \frac{X \boldsymbol{R}}{R^3} \right).$$

The Stokeslet velocity field, $\boldsymbol{U}_s$, corresponds to the viscous flow driven by point force $\boldsymbol{F}_0$.

3.2. *The outer solution*

The outer-region velocity and pressure can be presented as

$$\boldsymbol{u} = \epsilon \boldsymbol{U} + o(\epsilon), \qquad p = \epsilon^2 P + o(\epsilon^2).$$

The outer field, $\boldsymbol{U} = \left(U_x, U_y, U_z\right)$, is governed by Oseen-like equations and must match with Stokeslet velocity. Saffman (1965) showed that for the outer flow the particle is equivalent in the first approximation to the point force $\boldsymbol{F}_0$ being in the centre of the sphere. The matching condition can be encapsulated into the momentum equations by the introduction of a delta function. Then the first-order outer equations and boundary conditions can be written as

$$\nabla^2 \boldsymbol{U} - \nabla P - \overline{V}_x \frac{\partial \boldsymbol{U}}{\partial X} - \frac{\mathrm{d}\overline{V}_x}{\mathrm{d}Z} U_z \boldsymbol{e}_x = 6\pi V \boldsymbol{e}_x \delta(\boldsymbol{R}), \tag{3.6a}$$

$$\nabla \cdot \boldsymbol{U} = 0, \tag{3.6b}$$

$$\boldsymbol{U} = 0 \quad \text{on} \quad Z = -R_c^{1/2} d/l, \quad R_c^{1/2}\left(1 - d/l\right), \tag{3.6c}$$

$$\boldsymbol{U} = 0 \quad \text{as} \quad X \to \infty, \tag{3.6d}$$

where

$$\overline{V}_x = v + \gamma Z - 4 R_c^{-1/2} Z^2, \quad v = V R_c^{1/2}. \tag{3.7}$$

The outer problem is characterized by three independent dimensionless parameters: the channel Reynolds number R_c, the slip velocity V (or v) and the distance from the wall d/l (or γ). Hogg (1994) investigated the variation of the lift with R_c, d/l for two limiting cases $\epsilon^2 \ll v \ll 1$ (strong shear limit) and $v \gg 1$ (quiescent fluid) and channel Reynolds number less than 100. Below, its dependence on R_c, v, d/l is studied for large R_c.

To solve equations (3.6) we introduce the two-dimensional Fourier transforms of $\boldsymbol{U}$, P in the plane parallel to the channel walls:

$$\left\{ \begin{matrix} \widetilde{\boldsymbol{U}} \\ \widetilde{P} \end{matrix} \right\} = \frac{1}{4\pi^2} \int_{-\infty}^{\infty} \int_{-\infty}^{\infty} \left\{ \begin{matrix} \boldsymbol{U}(X, Y, Z) \\ P(X, Y, Z) \end{matrix} \right\} \mathrm{e}^{-\mathrm{i}(k_x X + k_y Y)} \mathrm{d}X \, \mathrm{d}Y.$$

Velocity and pressure fields are then given by the inverse Fourier transform:

$$\left\{ \begin{matrix} \boldsymbol{U} \\ P \end{matrix} \right\} = \int_{-\infty}^{\infty} \int_{-\infty}^{\infty} \left\{ \begin{matrix} \widetilde{\boldsymbol{U}}\left(k_x, k_y, Z\right) \\ \widetilde{P}\left(k_x, k_y, Z\right) \end{matrix} \right\} \mathrm{e}^{\mathrm{i}(k_x X + k_y Y)} \mathrm{d}k_x \, \mathrm{d}k_y.$$

Taking the Fourier transform of (3.6) one can obtain

$$\mathrm{L}\widetilde{\boldsymbol{U}} - \begin{pmatrix} \mathrm{i}k_x \\ \mathrm{i}k_y \\ \mathrm{d}/\mathrm{d}Z \end{pmatrix} \widetilde{P} - \mathrm{i}k_x \overline{V}_x \widetilde{\boldsymbol{U}} - \frac{\mathrm{d}\overline{V}_x}{\mathrm{d}Z} \widetilde{U}_z \boldsymbol{e}_x = \frac{3}{2\pi} V \delta(Z) \boldsymbol{e}_x, \tag{3.8a}$$

$$\mathrm{i}\left(k_x \widetilde{U}_x + k_y \widetilde{U}_y\right) + \mathrm{d}\widetilde{U}_z/\mathrm{d}Z = 0, \tag{3.8b}$$

$$\widetilde{\boldsymbol{U}} = 0 \quad \text{on} \quad Z = -R_c^{1/2} d/l, \quad R_c^{1/2}\left(1 - d/l\right), \tag{3.8c}$$

where

$$\mathrm{L} = \frac{\mathrm{d}^2}{\mathrm{d}Z^2} - k^2, \quad k^2 = k_x^2 + k_y^2.$$

Eliminating $\widetilde{U}_x, \widetilde{U}_y, \widetilde{P}$ in (3.8) one can derive the following fourth-order ordinary differential equation for the Fourier transform of the lateral component of the velocity:

$$\left(\mathrm{L}^2 - \mathrm{i}k_x \overline{V}_x \mathrm{L} - \mathrm{i}k_x 8 R_c^{-1/2}\right) \widetilde{U}_z = -\mathrm{i}k_x V \frac{3}{2\pi} \frac{\mathrm{d}\delta(Z)}{\mathrm{d}Z}, \tag{3.9a}$$

$$\widetilde{U}_z = \frac{\mathrm{d}\widetilde{U}_z}{\mathrm{d}Z} = 0 \quad \text{on} \quad Z = -R_c^{1/2} d/l, \quad R_c^{1/2}\left(1 - d/l\right). \tag{3.9b}$$

The term in the right-hand side is equivalent to a jump condition for the second derivative at the origin of coordinate system, so that

$$\left[\frac{\mathrm{d}^2 \widetilde{U}_z}{\mathrm{d}Z^2}\right] = -\mathrm{i}k_x V \frac{3}{2\pi}, \tag{3.10}$$

where $[f] = f(+0) - f(-0)$ is the magnitude of the jump.

The matching of outer field back to the inner flow requires the inner expansion (3.5) at $r \to \infty$ to be the same as the regular part of outer flow at the origin:

$$\boldsymbol{V}_1|_{r\to\infty} = [\boldsymbol{U} - \boldsymbol{U}_s]\,|_{R\to 0}.$$

Then the lift on a particle can be expressed in terms of the Fourier transform of the lateral velocity at the origin as (Saffman 1965)

$$F_{1z} = 6\pi V_{1z}|_{r\to\infty} = 6\pi\,\mathrm{Re}\left[\int_{-\infty}^{\infty}\int_{-\infty}^{\infty}\left(\widetilde{U}_z - \widetilde{U}_{zs}\right)|_{Z\to 0}\mathrm{d}k_x\,\mathrm{d}k_y\right]. \tag{3.11}$$

Here $\widetilde{U}_{zs}$ is the Fourier transform of the lateral component of the Stokeslet velocity field.

The equation (3.9) is solved numerically to calculate the Fourier transform of the lateral velocity at the origin. The numerical procedure is outlined in the Appendix. The numerical integration of the finite-difference version of (3.9) presents some difficulty at large channel Reynolds number. The routine numerical technique fails to converge in this case, since it does not resolve properly all the linearly independent solutions of the ordinary differential equation. As a result it is possible to calculate the lift only for channel Reynolds number less than approximately 100 (Schonberg & Hinch 1989; Hogg 1994). The problem is eliminated in the present work using the orthonormalization method (Godunov 1961; Conte 1966). This method is widely used

to solve linear stability problems (see, for example, Mack 1976; Shaqfeh & Acrivos 1987). It allows integrating (3.9) up to $k = 128$ over the entire interval R_c=100–3000. For greater k the asymptotic approximation (Hogg 1994)

$$\widetilde{U}_z\left(k_x,k_y,0\right) - \widetilde{U}_{zs}\left(k_x,k_y,0\right) = \gamma V \frac{3}{16\pi}\frac{k_x^2}{k^5} + O(k^{-5}) \quad \text{as} \quad k \to \infty, \tag{3.12}$$

is used. The numerical integration of (3.11) is done using plane polar coordinates k, $\theta = \arccos(k_x/k)$ instead of k_x, k_y. It can be verified directly from (3.9) that $\widetilde{U}_z\left(k_x,k_y,Z\right) = \widetilde{U}_z^*\left(-k_x,k_y,Z\right)$, where the superscript $*$ is used to denote the complex conjugated value, and $\widetilde{U}_z\left(k_x,k_y,Z\right) = \widetilde{U}_z\left(k_x,-k_y,Z\right)$. Thus it is sufficient to integrate (3.11) over the first quadrant.

The lift versus dimensionless distance from the wall d/l is shown in figure 2 by solid lines for various v and channel Reynolds numbers (*a*) $R_c = 100$, (*b*) 300, (*c*) 1000, (*d*) 3000. Some comments should be made on the applicability of the present analysis to the channel flow at $R_c = 3000$. The flow is assumed to be laminar although it may become turbulent at $R_c > R_{cr}^{'} \approx 2000$. However, $R_{cr}^{'}$ is the lowest bound for the laminar–turbulent transition. The critical Reynolds number may be raised if the perturbations of the flow at the channel inlet are minimized. The theoretical analysis of the linear-stability problem yields for channel flow $R_{cr} = 5772$ (Orszag 1971). Besides, the recent investigations by Asmolov & Manuilovich (1997, 1998) show that a small number of particles may stabilize the gas flow. To calculate the stability characteristics the effect of the inertial lift force on the momentum transfer between phases should be taken into account. So the study of the linear stability of dusty-gas flows is one possible field of application of the present study.

We present results only for the lower half of the channel flow, $0 \leqslant d/l \leqslant 0.5$, since the dependences are symmetrical with respect to the centreline. For the major portion of the channel the lift is positive, which means, for example, that if the particle leads the undisturbed flow and $V < 0$, it migrates toward the walls. The maximum value of the lift increases moderately with R_c for the range investigated, $100 < R_c < 3000$, while for lower magnitudes, $0.1 < R_c < 100$, it showed more rapid growth (Hogg 1994).

The lift varies rapidly close to the wall. This is due to the wall-induced inertia which is significant when the distance from the wall is of the order of the outer-region lengthscale, $l_p \sim lR_c^{-1/2}$, which decreases with R_c, and for greater Reynolds numbers the wall influence emerges only in thin layers near the walls. It is of interest to compare the lift in the near-wall regions with the predictions of Cox & Hsu (1977) and McLaughlin (1993).

Cox & Hsu (1977) considered the sedimentation of a small sphere in a vertical parabolic flow. The distance from the wall was assumed to be much greater than the sphere radius and much less than the outer-region lengthscale, that is the wall lies within the inner region. The particle is also treated as a point force. It follows from their analysis that the force, written in the present notation, is

$$F_{1z} = \pi V\left[\frac{9}{16}v + \frac{3}{16}\frac{d}{l_p}\left(22 - 105\frac{d}{l_p}R_c^{-1/2}\right)\right]. \tag{3.13}$$

Asmolov (1989, 1990) and McLaughlin (1993) considered the inertial migration of a particle translating in a linear shear flow, bounded by a single wall. The distance from the wall was assumed to be of the order of the lengthscale of the outer region, l_G, and the ratio of the two parts of the undisturbed velocity corresponding to uniform flow

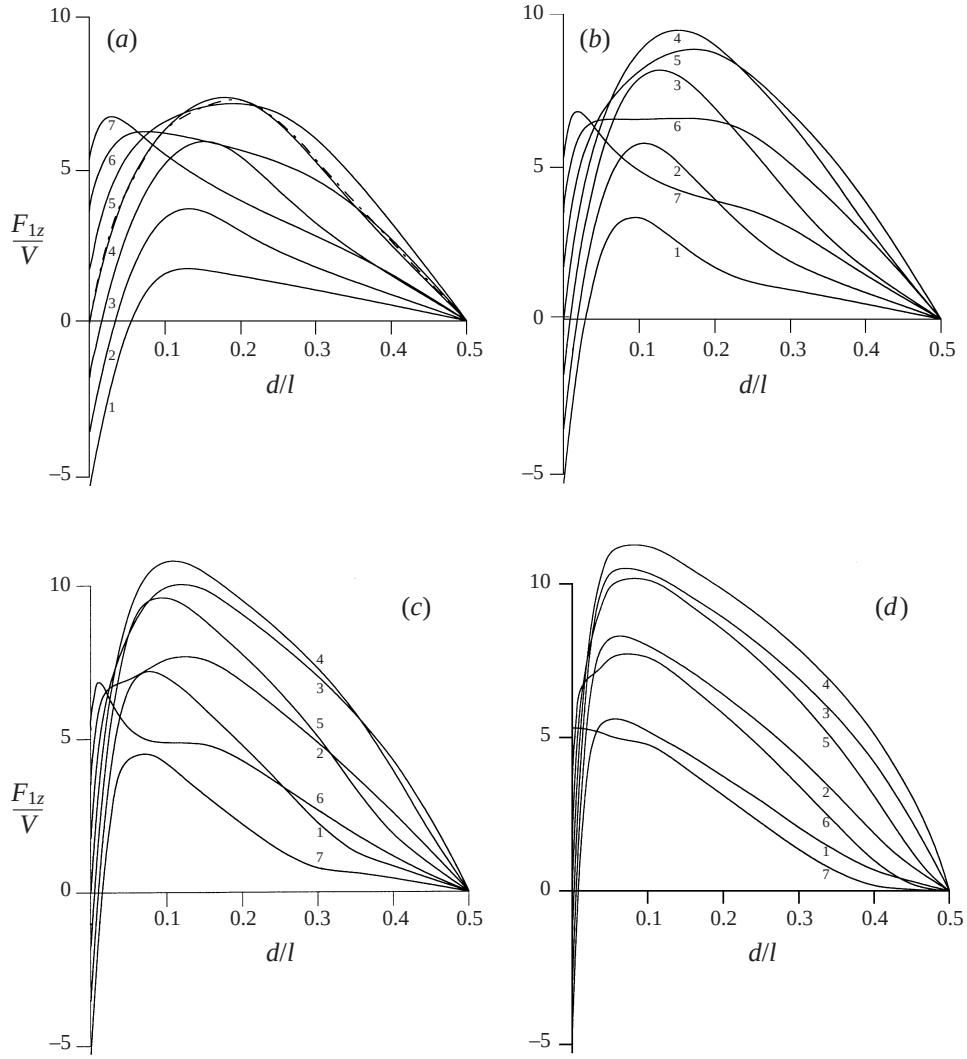

FIGURE 2. Lift on a non-neutrally buoyant particle versus its position d/l for (*a*) $R_c = 100$, (*b*) 300, (*c*) 1000, (*d*) 3000. Parameter $v = VR_c^{1/2}$ changes from -3 to 3 with step 1 (curves 1–7 respectively). (*a*) Dashed-and-dotted line represents the lift calculated by Hogg (1994) at $\epsilon^2 \ll v \ll 1$ (strong shear limit), $R_c = 100$ (compare with curve 4).

and the shear, $\alpha = R_V/R_G^{1/2}$, of the order of unity. A method similar to that presented here was used to deduce the outer-flow equations. The analytical solution for the lift in terms of integrals of Airy functions was obtained. The migration velocity, $v_m = F_{1z}/6\pi$, may be divided into two parts (McLaughlin 1993), so that

$$v_m = v_m^u + v_m^w.$$

Here v_m^u denotes the inertial migration velocity in an unbounded fluid, and v_m^w is the disturbance created by the wall. The first term depends only on α. The second term, v_m^w, depends on α and dimensionless distance from the wall, d/l_G. McLaughlin (1993) showed that for distances small compared with l_G the results derived for linear shear flow reduce to those of Cox & Hsu (1977).

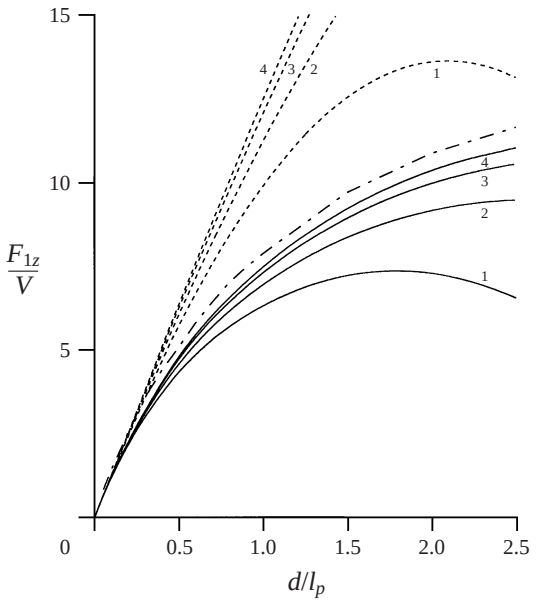

FIGURE 3. Lift on a non-neutrally buoyant particle versus d/l_p (solid lines) for $\epsilon^2 \ll v \ll 1$ (strong shear regime) in comparison with that calculated by Cox & Hsu (1977) (dashed lines) and by McLaughlin (1993) (dashed-and-dotted line). Curves 1–4 correspond to $R_c = 100, 300, 1000, 3000$.

The results of the present work must also reduce to (3.13) for $d/l_p \ll 1$ since the inertial terms in (3.6 *a*) are again small compared with the viscous ones. Moreover, at large channel Reynolds number and $d/l_p = O(1)$ they must tend to the values appropriate to the linear shear flow, since effects due to both the second far-removed wall and the curvature of undisturbed velocity profile (the last term in (3.7)) become negligible as $R_c \to \infty$. In order to illustrate this effect the lift for a strong shear regime is presented in figure 3 as a function of distance from the wall scaled by l_p. For comparison the results of Cox & Hsu (1977) and McLaughlin (1993) are also plotted. The lift in the near-wall regions converges to the linear-shear predictions at large Reynolds numbers, and to the Cox–Hsu theory for small d/l_p. However, the deviation grows with d/l_p and remains sizeable even for $R_c = 3000$. It cannot be explained by the wall effect, since the wall-induced inertia decreases with the distance from the wall, but only by the curvature of the undisturbed velocity profile.

Following the approach of McLaughlin (1993) the lift on a sphere in a channel flow can also be presented as the sum of the lift in unbounded parabolic flow, F_{1z}^u, and the disturbance created by the wall, F_{1z}^w. Such a breakdown is rather unconventional, since an unbounded parabolic velocity profile cannot be realized, but it permits the separation of the effects due to the curvature of the undisturbed velocity profile and the wall-induced inertia. It follows from the above comparison of channel-flow and linear-shear migration that the wall contributions for the two cases are close, while the unbounded lift forces are different even at large channel Reynolds number. Note that for a major portion of the channel flow, excluding thin layers near the walls, the distance from the wall is large compared with l_p. In this region the wall effect is small, and the lift is close to F_{1z}^u. This limit can be demonstrated more clearly if one uses l_G to scale the outer-flow equations. The analysis based on this scaling is developed in the next section.

The lift always vanishes at the channel centre because of the symmetry of the flow.

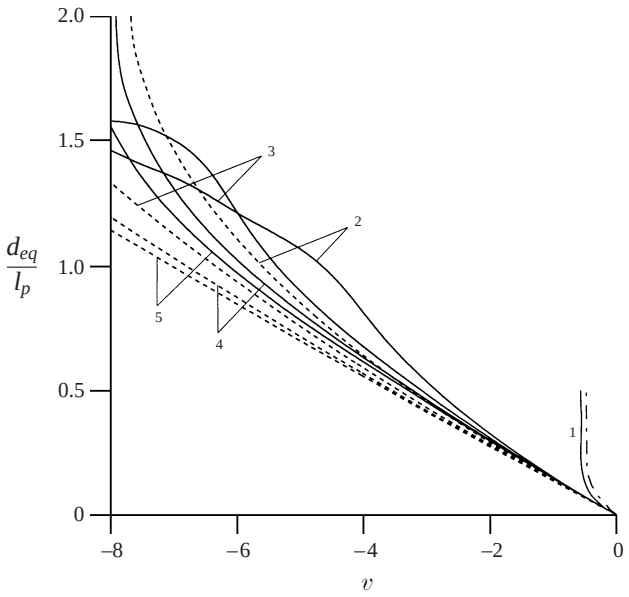

FIGURE 4. The equilibrium position nearest to the wall, d_{eq}/l_p versus v. Curves 1–5 correspond to $R_c = 1$, 100, 300, 1000, 3000. The dashed lines are the predictions of Cox–Hsu theory, following from (3.13). The dashed-and-dotted line presents the results of Hogg (1994) for $R_c = 1$.

For a particle leading the undisturbed flow, when $V < 0$, this equilibrium position is unstable, while for $V > 0$ it is stable. The particle has a stable equilibrium position near the wall for $v < 0$. The equilibrium position nearest to the wall, d_{eq}, scaled by l_p is presented in figure 4 as a function of v. The slip velocity for which the lift vanishes at given d_{eq} is evaluated using the Newton method. Hogg (1994) calculated the variation of d_{eq} for $R_c = 1$. He showed that the equilibrium position exists for limited range of slip velocity, $v_{\min} \leqslant v \leqslant 0$, where $v_{\min} \approx -0.50$. We recalculate these results and obtain slightly greater values of minimum slip velocity, $v_{\min} \approx -0.56$. For large channel Reynolds numbers the equilibrium position occurs within more wide range of v. For $-2 \leqslant v \leqslant 0$ it may be predicted well by Cox & Hsu's (1977) theory.

Extra equilibrium positions across the channel width may arise for large $|v|$. The lift at $v = 8$, -8 and various R_c is presented as a function of d/l in figure 5. Two additional equilibrium positions arise at $v = \pm 8$, $R_c = 3000$ and $v = 8$, $R_c = 1000$. Note that the magnitude of the lift at large slip velocity is many times smaller than that for $v = O(1)$. This effect was pointed out by McLaughlin (1991) for unbounded linear shear flow. For $\alpha \gg 1$ the lengthscale of the region where the convective terms balance the viscous ones is the Oseen length, $l_s = v/V' \ll l_p$. In this region the term involving v is larger than the other convective terms, and the disturbance flow is close to axisymmetric Oseen flow. This gives no lift on a sphere. The shear convective term becomes of the same order as the uniform one at distances of order l_p/α where the disturbance flow is very small. As a result the lift rapidly decreases as $\alpha \to \infty$.

Similar reasoning may be applied for a particle translating with large slip velocity in a channel flow. The numerical calculations show that the main contribution to the lateral velocity at the origin at high slip velocities comes from the small values of k. This means that the lift is due to the flow disturbances with the characteristic length, $l_p/|v|$, large compared even with l_p. For such disturbances the wall effect

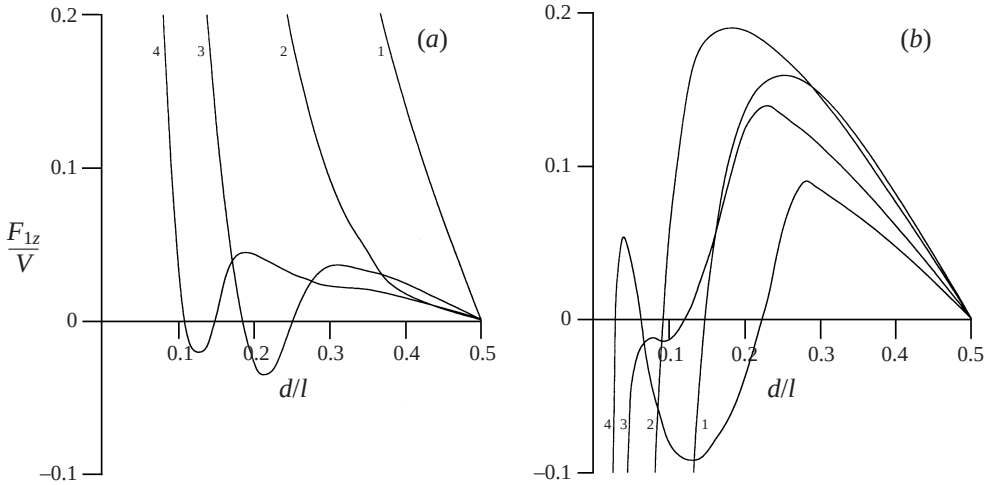

FIGURE 5. Lift on a non-neutrally buoyant particle at large $|v|$ and $R_c = 100, 300, 1000, 3000$ (curves 1–4 respectively). (*a*) For $v = 8$ one (curves 1, 2) or three (curves 3, 4) equilibrium positions may exist. (*b*) For $v = -8$ the dependences may have two (curves 1–3) or four zeros (curve 4).

remains sizeable, and this may explain the emerging of extra equilibrium positions with increasing channel Reynolds numbers.

4. Solution for non-neutrally buoyant particle based on the l_G lengthscale

The velocity and pressure fields and the force on a sphere are sought again in the form of series in a small parameter, but instead of ϵ a new asymptotic parameter $\epsilon_G = R_G^{1/2} = \gamma^{1/2}\epsilon$ is used. The dimensionless force on a sphere is $\boldsymbol{F} = 6\pi V \boldsymbol{e}_x + \epsilon_G \boldsymbol{F}_G$. The dimensionless undisturbed velocity can be rewritten in terms of ϵ_G as

$$\overline{\boldsymbol{v}} = \left(V + z\epsilon_G \gamma^{1/2} R_c^{-1/2} - 4z^2 \epsilon_G^2 \gamma^{-1} R_c^{-1}\right) \boldsymbol{e}_x. \tag{4.1}$$

The new outer normal coordinate is defined as $\zeta = z\epsilon_G = Z\gamma^{1/2}$. The two-dimensional Fourier transforms of velocity, $\boldsymbol{\Gamma}\left(\zeta, q_x, q_y\right)$, and pressure, $\Pi\left(\zeta, q_x, q_y\right)$, are introduced similarly to (3.8). As a result one can obtain the following equation for the Fourier transform Γ_z of the lateral component of the velocity:

$$\left(\mathrm{L}_G^2 - \mathrm{i}q_x \overline{V}_{Gx} \mathrm{L}_G - \mathrm{i}q_x 2\sigma\right) \Gamma_z = -\mathrm{i}q_x V \frac{3}{2\pi} \frac{\mathrm{d}\delta(\zeta)}{\mathrm{d}\zeta}, \tag{4.2a}$$

$$\Gamma_z = \frac{\mathrm{d}\Gamma_z}{\mathrm{d}\zeta} = 0 \quad \text{on} \quad \zeta = -\gamma^{1/2} R_c^{1/2} d/l, \quad \gamma^{1/2} R_c^{1/2} \left(1 - d/l\right). \tag{4.2b}$$

Here $\mathrm{L}_G = \mathrm{d}^2/\mathrm{d}\zeta^2 - q^2$, and $\overline{V}_{Gx}$ is the undisturbed velocity profile written in terms of ζ. In view of (4.1) it is given by

$$\overline{V}_{Gx} = \alpha + \zeta - \sigma\zeta^2,$$

where

$$\alpha = V'(vG)^{-1/2} = V\gamma^{-1/2} R_c^{1/2}, \quad \sigma = 4\gamma^{-3/2} R_c^{-1/2}. \tag{4.3}$$

The equations (4.2) are very similar to (3.9). The main difference is that $\overline{V}_{Gx}$ contains only two dimensionless groups instead of the three occurring in $\overline{V}_x$. The third

group, R_c, occurs only in the boundary conditions (4.2 *b*). R_c, α, σ are taken as the main independent parameters characterizing the inertial migration in terms of the l_G lengthscale. Other groups, γ and the distance from the wall, in view of (4.3), can be expressed in terms of the main ones as

$$\gamma = \left(4\sigma^{-1}R_c^{-1/2}\right)^{2/3}, \qquad \frac{d}{l} = \frac{1}{2} - \frac{1}{8}\left(4\sigma^{-1}R_c^{-1/2}\right)^{2/3}, \tag{4.4a,b}$$

$$\frac{d}{l_G} = \left(4\sigma^{-1}R_c\right)^{1/3}\left[\frac{1}{2} - \frac{1}{8}\left(4\sigma^{-1}R_c^{-1/2}\right)^{2/3}\right]. \tag{4.4c}$$

New dimensionless groups, α and σ, characterize the magnitudes of the uniform and parabolic flows relative to the linear one in the undisturbed velocity. The first group, α, may be arbitrary. For the second one we have from (4.3) $\sigma \geqslant R_c^{-1/2}/2$, since γ reaches its maximum value, $\gamma_w = 4$, on the wall. α and σ tend to infinity as the particle moves to the centreline where $\gamma \to 0$. The magnitude of σ characterizes for given R_c not only the curvature of the undisturbed velocity profile but also the distance from the wall. For this reason one can expect that the lift calculated at different R_c would be close in value for sufficiently large σ when the wall effect becomes insignificant.

The numerical procedure used to calculate the lateral velocity at the origin is similar to that described in § 3. In figure 6 the lift coefficient, introduced by $c_s = F_{Gz}/V$, is presented as a function of σ. For comparison the lift force in the linear-shear flow bounded by a single wall (McLaughlin 1993) and their asymptotes corresponding to the unbounded case (Asmolov 1990; McLaughlin 1991) are also shown in the figure by dashed-and-dotted and dashed lines respectively. In this case σ is treated as characterizing only the distance from the wall. The dependence on d/l_G is converted to σ-dependences for different R_c using (4.4).

It is seen that for small σ the lift is close to that in the linear-shear flow. In this region the wall effect is dominant. For greater σ or, equivalently, for greater distance from the wall the wall-induced inertia is insignificant, and the dependences obtained for various R_c are very close. They tend to the values which correspond to the lift coefficient in the unbounded parabolic flow, c_s^u, which differs from that in the unbounded linear-shear flow (dashed line) even when the curvature is sufficiently small, $\sigma \leqslant 0.1$. c_s^u is a function of only two dimensionless groups α, σ, instead of the three, R_c, v, γ, used above.

4.1. *Lift in unbounded parabolic flow*

The Fourier transform Γ_z^u of the lateral component of the velocity for the unbounded problem is governed by (4.2 *a*) with the boundary conditions

$$\Gamma_z^u \to 0 \quad \text{as} \quad \zeta \to \infty. \tag{4.5}$$

To obtain the numerical solution in this case the modification of orthonormalization method proposed by Mack (1976) is used. The boundaries of the integration domain are set at sufficiently large distance $|\zeta|$ from the sphere where the analytical expressions for linearly independent solutions $\varphi_i(\zeta)$, $i = 1$–4 can be found. Assuming $\varphi_i = \exp\left(\lambda_i |\zeta|^{\nu_i}\right)$ one can obtain for two solutions decaying with $|\zeta|$

$$\varphi_1 = \exp\left(-q|\zeta|\right), \ \varphi_2 = \exp\left(-(\mathrm{i}\sigma q_x)^{1/2}\zeta^2/2\right) \qquad \text{as} \quad \zeta \to \infty, \ q = O(1),$$

where the branch of $(\mathrm{i})^{1/2}$ is chosen with a positive real part.

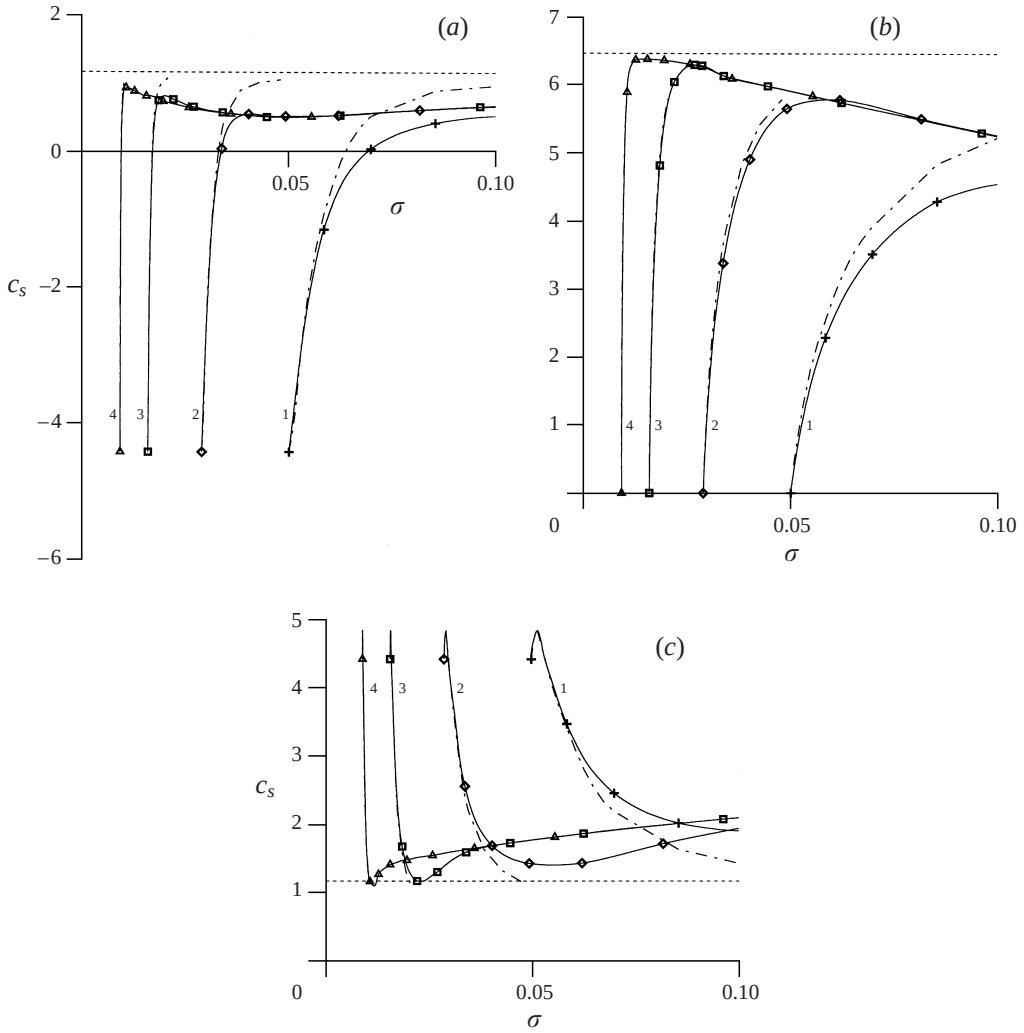

FIGURE 6. Lift coefficient as a function of σ for (*a*) $\alpha = -2.5$, (*b*) $\epsilon^2 \ll \alpha \ll 1$, (*c*) $\alpha = 2.5$, and $R_c = 100, 300, 1000, 3000$ (curves 1–4 respectively). Symbols on the curves correspond to the particle position (from left to right) $d/l = 0,\ 0.05,\ 0.1,\ 0.15, \ldots$. The dashed-and-dotted lines are the lift in the linear shear flow bounded by a single wall (McLaughlin 1993), and the dashed lines are their asymptotes corresponding to the unbounded case (Asmolov 1990; McLaughlin 1991).

The calculations of the lift coefficient in unbounded parabolic flow, c_s^u, for the case $\sigma = 0$ which corresponds to linear shear flow, show very close agreement with predictions by Asmolov (1990) and McLaughlin (1991).

Figure 7 shows the dependence of c_s^u on α for various σ. The maximum value of the lift in the parabolic flow is less than that in the linear shear case and reduces with σ. However, for large magnitudes of the slip velocity the reverse situation takes place, and the lift in the unbounded parabolic flow is many times greater than that for the linear shear case. As a result the lift decay with $|\alpha|$ is not so rapid as for the linear shear. The values of c_s^u are given in table 1 for several values of σ.

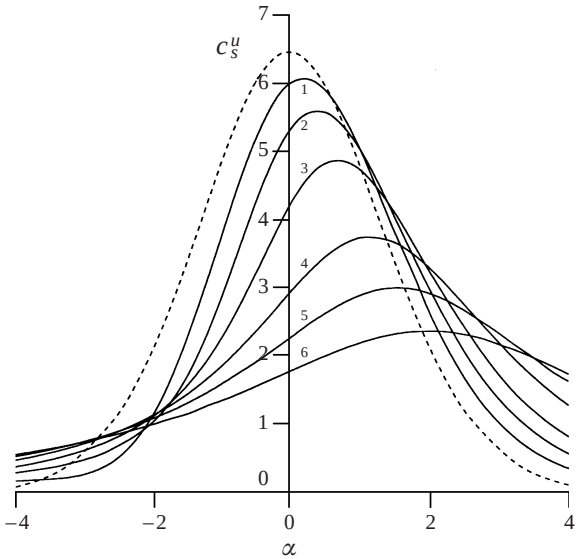

FIGURE 7. Lift coefficient for a non-neutrally buoyant particle in unbounded parabolic flow versus α and various $\sigma = 0.05$, 0.1, 0.2, 0.5, 1, 2 (curves 1–6 respectively). Dashed line represents the lift in unbounded linear shear flow (Asmolov 1990; McLaughlin 1991), $\sigma = 0$.

α	$\sigma = 0.0$	0.05	0.1	0.2	0.3	0.4	0.5	0.75	1.0	2.0	4.0
−4.0	0.082	0.170	0.289	0.379	0.434	0.460	0.477	0.504	0.530	0.557	0.470
−3.5	0.242	0.194	0.362	0.479	0.537	0.564	0.580	0.603	0.626	0.640	0.526
−3.0	0.557	0.267	0.482	0.619	0.677	0.701	0.716	0.727	0.746	0.739	0.591
−2.5	1.124	0.526	0.692	0.821	0.870	0.885	0.894	0.886	0.896	0.858	0.665
−2.0	2.039	1.155	1.042	1.118	1.141	1.136	1.131	1.089	1.082	0.995	0.749
−1.5	3.309	2.289	1.724	1.578	1.527	1.478	1.445	1.348	1.312	1.146	0.843
−1.0	4.744	3.768	2.879	2.272	2.068	1.938	1.854	1.671	1.592	1.344	0.947
−0.5	5.949	5.171	4.260	3.227	2.781	2.525	2.365	2.058	1.909	1.552	1.059
0.0	6.462	5.991	5.308	4.223	3.576	3.185	2.938	2.485	2.261	1.771	1.175
0.5	5.949	5.919	5.578	4.817	4.193	3.750	3.453	2.890	2.615	1.986	1.292
1.0	4.744	5.072	5.057	4.743	4.351	3.999	3.732	3.172	2.876	2.172	1.399
1.5	3.309	3.843	4.066	4.126	4.005	3.827	3.668	3.237	2.984	2.299	1.489
2.0	2.039	2.630	2.982	3.249	3.343	3.331	3.294	3.063	2.900	2.341	1.550
2.5	1.124	1.656	2.042	2.411	2.600	2.695	2.740	2.707	2.651	2.290	1.574
3.0	0.557	0.989	1.339	1.694	1.931	2.076	2.170	2.269	2.307	2.141	1.558
3.5	0.242	0.571	0.856	1.163	1.397	1.551	1.661	1.831	1.943	1.943	1.503
4.0	0.082	0.323	0.539	0.788	1.001	1.142	1.247	1.443	1.599	1.702	1.415

TABLE 1. Lift coefficient c_s^u for a non-neutrally buoyant particle in unbounded parabolic flow.

5. Neutrally buoyant particle

The approach used in this section to derive the outer-flow governing equations is similar to the analysis of Schonberg & Hinch (1989). The difference is that we use $\epsilon = R_p^{1/2}$ as the main asymptotic parameter instead of $a/l = R_p^{1/2} R_c^{-1/2}$. For the neutrally buoyant sphere, when $|V| \ll \epsilon^2/R_c$, the flow disturbance is due to the shear on the sphere. The expansions for $\boldsymbol{u}$ and p can be presented as

$$\boldsymbol{u} = \epsilon \boldsymbol{u}_0^{nb} + o(\epsilon), \qquad p = \epsilon p_0^{nb} + o(\epsilon). \tag{5.1}$$

Governing equations for the main-order inner solution remain the creeping-flow equations (3.2 *a*, *b*) while the boundary conditions in this case are

$$\boldsymbol{u}_0^{nb}=R_c^{-1/2}\left(\boldsymbol{\Omega}_p\wedge\boldsymbol{r}-\gamma z\boldsymbol{e}_x\right)\quad\text{on}\quad r=1, \tag{5.2a}$$

$$\boldsymbol{u}_0^{nb}\to 0\quad\text{as}\quad r\to\infty. \tag{5.2b}$$

Note that the main-order boundary conditions are independent of the curvature of the undisturbed velocity profile. Solution of (3.2 *a*, *b*), (5.2 *a*, *b*) is given by

$$\boldsymbol{u}_0^{nb}=R_c^{-1/2}\left[\left(\boldsymbol{\Omega}_p+\frac{\gamma}{2}\boldsymbol{e}_y\right)\wedge\frac{\boldsymbol{r}}{r^3}+\frac{5}{2}\gamma\boldsymbol{r}xz\left(\frac{1}{r^7}-\frac{1}{r^5}\right)-\frac{\gamma}{2r^5}\left(\boldsymbol{e}_x z+\boldsymbol{e}_z x\right)\right]. \tag{5.3}$$

This velocity field results in a couple on the sphere $8\pi R_c^{-1/2}\left(\boldsymbol{\Omega}_p+\boldsymbol{e}_y\gamma/2\right)$ but no force. Since there is no torque on the sphere we have for the particle angular velocity $\boldsymbol{\Omega}_p=-\boldsymbol{e}_y\gamma/2$, and the first term in square brackets in (5.3) equals zero.

When written in outer variables (5.3) gives for torque-free particle

$$\boldsymbol{u}_0^{nb}=-\epsilon^2\frac{5}{2}R_c^{-1/2}\frac{\gamma\boldsymbol{R}XZ}{R^5}+O(\epsilon^4). \tag{5.4}$$

The main-order term in the last expansion is the strainlet velocity field. It corresponds to viscous flow driven by a symmetric force dipole.

The outer-region velocity and pressure fields in view of (5.1) and (5.4) are presented as

$$\boldsymbol{u}=\epsilon^3\boldsymbol{U}+o(\epsilon^3),\qquad p=\epsilon^4P+o(\epsilon^2).$$

Following Saffman (1965) and Schonberg & Hinch (1989), the matching condition can be encapsulated into the momentum equations by the introduction of singularity corresponding to the symmetric force dipole. Then the equations governing the outer flow are

$$\nabla^2\boldsymbol{U}-\nabla P-\overline{V}_x\frac{\partial\boldsymbol{U}}{\partial X}-\frac{\mathrm{d}\overline{V}_x}{\mathrm{d}Z}W\boldsymbol{e}_x=\frac{10}{3}\pi\gamma R_c^{-1/2}\left[\boldsymbol{e}_x\frac{\partial\delta\left(\boldsymbol{R}\right)}{\partial Z}+\boldsymbol{e}_z\frac{\partial\delta\left(\boldsymbol{R}\right)}{\partial X}\right], \tag{5.5}$$

together with the equation of continuity and boundary conditions (3.6 *c*, *d*). Note that in (5.5) $\overline{V}_x=\gamma Z-4R_c^{-1/2}Z^2$ since in this case $V=0$. The system obtained can be reduced to the following fourth-order ordinary equation for the Fourier transform of the lateral velocity:

$$\left(\mathrm{L}^2-\mathrm{i}k_x\overline{V}_x\mathrm{L}-\mathrm{i}k_x 8R_c^{-1/2}\right)\widetilde{U}_z=\mathrm{i}k_x\gamma R_c^{-1/2}\frac{5}{6\pi}\left[\frac{\mathrm{d}^2\delta(Z)}{\mathrm{d}Z^2}+k^2\delta(Z)\right], \tag{5.6}$$

with the boundary conditions (3.9*b*). The term in the right-hand side is equivalent to the jump conditions for the first and third derivatives at the origin of the coordinate system, so that

$$\left[\frac{\mathrm{d}\widetilde{U}_z}{\mathrm{d}Z}\right]=\mathrm{i}k_x\gamma R_c^{-1/2}\frac{5}{6\pi},$$

$$\left[\frac{\mathrm{d}^3\widetilde{U}_z}{\mathrm{d}Z^3}\right]=\left[2k^2+\mathrm{i}k_x\overline{V}_x(0)\right]\left[\frac{\mathrm{d}\widetilde{U}_z}{\mathrm{d}Z}\right]+\mathrm{i}k_xk^2\gamma R_c^{-1/2}\frac{5}{6\pi}=\mathrm{i}k_xk^2\gamma R_c^{-1/2}\frac{5}{2\pi}.$$

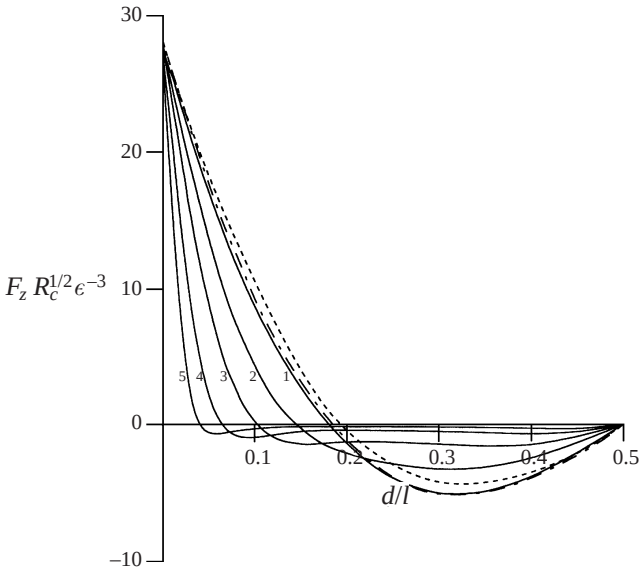

FIGURE 8. Lift on a neutrally buoyant particle for $R_c = 15$, 100, 300, 1000, 3000 (curves 1–5). Dashed-and-dotted line is the lift evaluated by Schonberg & Hinch (1989) for $R_c = 15$, and dashed line represents the predictions of Vasseur–Cox (1976) theory.

Since the Fourier transform of the lateral component of the strainlet velocity field is purely imaginary, the lift on a particle can be expressed as

$$F_z = 6\pi\epsilon^3 \,\mathrm{Re}\left[\int_{-\infty}^{\infty}\int_{-\infty}^{\infty} \widetilde{U}_z\Big|_{Z\to 0}\,\mathrm{d}k_x\,\mathrm{d}k_y\right].$$

The lateral velocity at the origin is evaluated using the same numerical procedure as that described in § 3. To approximate $\widetilde{U}_z$ at large Fourier mode number the asymptotic approach based on (A 3) is used. It yields for a neutrally buoyant sphere

$$\mathrm{Re}\,\widetilde{U}_z\left(k_x,k_y,0\right) = \gamma R_c^{-1}\frac{15}{8\pi}\frac{k_x^2}{k^5} + O(k^{-5}) \quad \text{as} \quad k\to\infty.$$

The results are shown in figure 8. The lift on a neutrally buoyant particle is presented as a function of particle position in the channel, d/l, for various Reynolds numbers, $15 \leqslant R_c \leqslant 3000$. For $R_c = 15$ the lift is in good agreement with that calculated by Schonberg & Hinch (1989) and close to the Vasseur–Cox prediction obtained under the assumption $R_c \ll 1$, when the walls lie within the inner region. It can be seen again that at large Reynolds numbers the wall effect emerges in a thin layer near the wall. In the remainder of the channel flow, where the wall influence is negligible, the magnitude of the lift is significantly less and decreases with Reynolds number.

The equilibrium position of a neutrally buoyant sphere, d_{eq}/l_p, versus R_c is presented in figure 9. The Reynolds number for which the lift vanishes at given d_{eq} is evaluated using the Newton method.

6. Solution for a neutrally buoyant particle via the l_G lengthscale

In order to separate the effects of the curvature of the unperturbed velocity profile and wall-induced inertia the outer flow past a neutrally buoyant sphere is considered

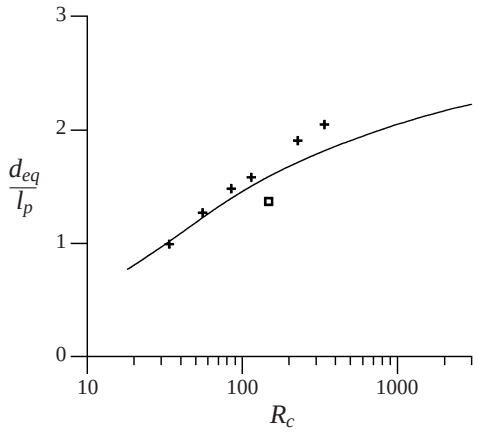

FIGURE 9. The equilibrium position of a neutrally buoyant particle versus the channel Reynolds number in comparison with experimental results of Segré & Silberberg (1962) (+) and extrapolation of Schonberg & Hinch (1989) from the partial profile of migration velocity (□).

in terms of the local shear rate, G. The disturbance velocity is scaled by $U'_G = (\nu G)^{1/2}$ instead of U'_m, and the space coordinates by l_G. The main-order dimensionless force on a sphere is $F_z = \epsilon_G^3 c_{nb} \boldsymbol{e}_z$. Hence, the dimensional force is expressed in terms of lift coefficient, c_{nb}, as

$$\boldsymbol{F}' = \rho G^2 a^4 c_{nb} \boldsymbol{e}_z.$$

6.1. *Channel flow*

Similarly to (5.6) one can obtain the following equation governing the Fourier transform Γ_z of the lateral velocity:

$$\left(\mathrm{L}_G^2 - \mathrm{i}q_x \overline{V}_{Gx} \mathrm{L}_G - \mathrm{i}q_x 2\sigma\right) \Gamma_z = \mathrm{i}q_x \frac{5}{6\pi} \left[\frac{\mathrm{d}^2\delta(\zeta)}{\mathrm{d}\zeta^2} + q^2\delta(\zeta)\right]. \tag{6.1}$$

The boundary conditions for (6.1) are (4.2 *b*), and the unperturbed velocity is given by

$$\overline{V}_{Gx} = \zeta - \sigma\zeta^2. \tag{6.2}$$

The dependence of the lift coefficient on the curvature, calculated for various Reynolds numbers and presented in figure 10, is very similar to the non-neutrally buoyant case. It also converges, to the limiting dependence, c_{nb}^u, corresponding to the unbounded parabolic flow. As the uniform flow in the unperturbed velocity profile is zero for the neutrally buoyant particle (see equation (6.2)), c_{nb}^u depends on only one dimensionless group, namely, σ.

To evaluate the lift in unbounded parabolic flow we solve the equation (6.1) together with the boundary conditions (4.5). The numerical procedure used to calculate c_{nb}^u is the same as that described in § 4.1. Figure 11 shows the lift on a neutrally buoyant sphere in unbounded flow versus σ. The magnitude of the lift grows monotonically with σ. It equals zero at $\sigma = 0$ (unbounded linear-shear flow) because of the symmetry of the flow.

6.2. *Linear-shear flow bounded by a single wall* ($\sigma = 0$)

The lift on a neutrally buoyant sphere in linear shear flow ($\sigma = 0$) results from the wall effect only. The Fourier transform of the lateral velocity again satisfies equation

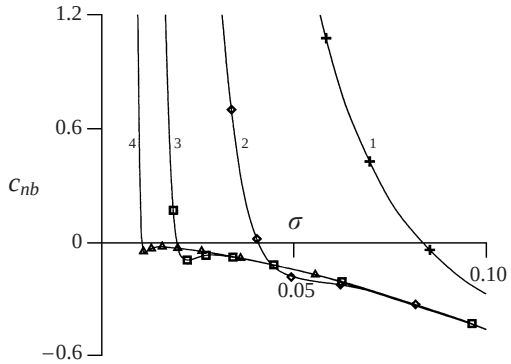

FIGURE 10. Lift coefficient for a neutrally buoyant particle as a function of σ for $R_c = 100$, 300, 1000, 3000 (curves 1–4 respectively). Symbols on the curves correspond to the particle position (from left to right) $d/l = 0.05,\ 0.1,\ 0.15, \ldots$.

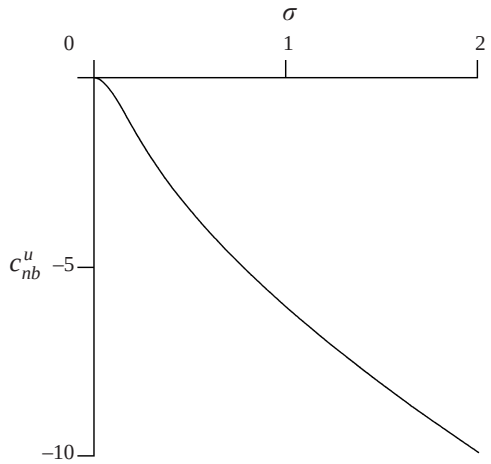

FIGURE 11. Lift coefficient for a neutrally buoyant particle in unbounded parabolic flow.

(6.1) with the undisturbed velocity, $\overline{V}_{Gx} = \zeta$. The boundary conditions in this case are

$$\Gamma_z = \frac{\mathrm{d}\Gamma_z}{\mathrm{d}\zeta} = 0 \quad \text{on} \quad \zeta = -\zeta_w < 0,$$

$$\Gamma_z \to 0 \quad \text{as} \quad \zeta \to +\infty.$$

Here ζ_w is the dimensionless distance from the wall.

The upper boundary of the integration domain is set similarly to § 4.1 at sufficiently large ζ where the analytical expressions for linearly independent solutions $\varphi_i(\zeta)$, $i = 1$–4 can be found. Assuming that $\varphi_i = \exp(\lambda_i \zeta^{\nu_i})$ one can obtain for the decaying solutions:

$$\varphi_1 = \exp(-q\zeta),\ \varphi_2 = \exp\left(-\tfrac{2}{3}(\mathrm{i}q_x)^{1/2}\zeta^{3/2}\right) \quad \text{as} \quad \zeta \to +\infty,\ q = O(1),$$

where the branch of $i^{1/2}$ is chosen with a positive real part.

The c_{nb} dependence on ζ_w is presented in figure 12. The lift is positive for all ζ_w, i.e. the particle always migrates outward from the wall. There is no equilibrium position for a neutrally buoyant particle in a linear shear flow bounded by a single wall.

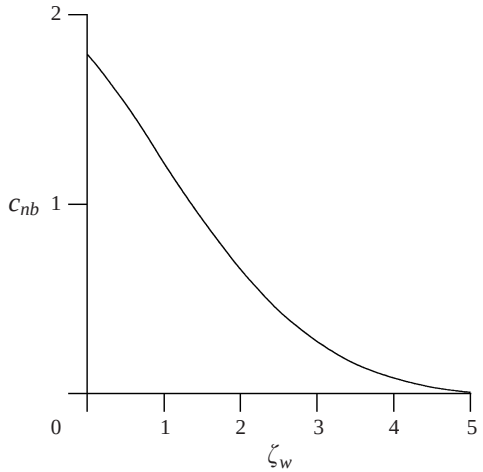

FIGURE 12. Lift coefficient for a neutrally buoyant particle in a linear shear flow bounded by a single wall.

7. Comparison with experiments

The results of two experimental investigations (Segré & Silberberg 1962*b*; Jeffrey & Pearson 1965) relevant to those of present work are compared with the theoretical predictions. Jeffrey & Pearson (1965) studied the migration of dense particles in upward and downward Poiseuille flow in a vertical pipe with Reynolds number R_c varied from 42 to 230. The particle Reynolds number, R_p, was in the range from 0.02 to 0.5. Hogg (1994) compared two sets of experimental data for downward flow with $R_c = 90.6$, $v = 0.379$ and $R_c = 178$, $v = 0.27$. However, he did not describe in detail how the effect of uniform flow was taken into account in the outer-flow equations. We recalculate the lift for the same values of dimensionless groups, R_c, v. The results are presented in figure 13(*a*). The dependences differ significantly from those calculated by Hogg. However, all theoretical predictions agree only qualitatively with experimental values.

Schonberg & Hinch (1989) compared the equilibrium positions for neutrally buoyant particles evaluated theoretically with the experimental data of Segré & Silberberg (1962*b*). Very good agreement was demonstrated for channel Reynolds numbers less than 75. For $R_c = 150$ the equilibrium positions were found approximately by extrapolating the partial profile of migration velocity.

We compare not only the equilibrium positions for a neutrally buoyant particle at large channel Reynolds number, but also the value of the lift. The calculated equilibrium positions are very close both to experimental (Segré & Silberberg 1962*b*) and theoretical (Schonberg & Hinch 1989) results for $R_c \leqslant 100$ (see figure 10). For larger Reynolds numbers they deviate from experimental results. However, agreement with the experiments is better than the extrapolation of the partial profile of the lift that Schonberg & Hinch gave for $R_c = 150$.

The comparison of the lift on neutrally buoyant particle versus particle position between theoretical predictions of the present work and experimental results of Segré & Silberberg (1962*b*) is illustrated in figure 13(*b*). They agree well except for the particles near the centreline.

Two possible reasons for the discrepancy between theoretical and experimental results were pointed out by Schonberg & Hinch (1989) and Hogg (1994). First, it may

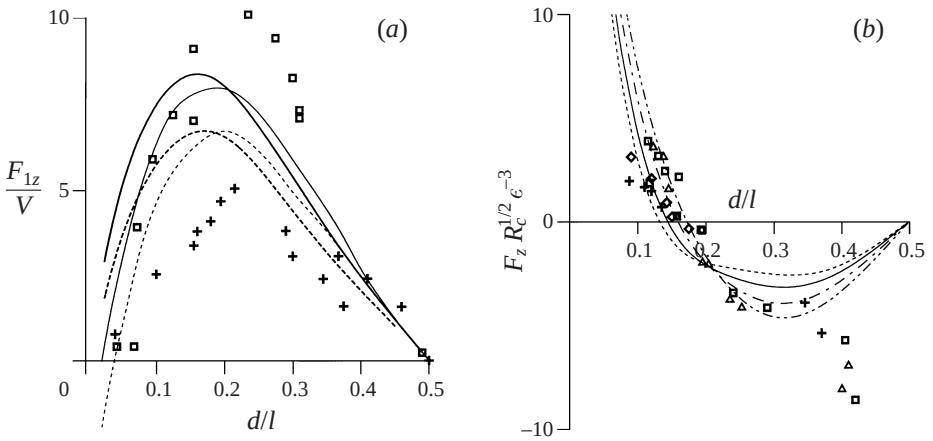

FIGURE 13. Comparison of theoretical predictions of the lift on (*a*) non-neutrally buoyant and (*b*) neutrally buoyant particles with experimental results. (*a*) $R_c = 90.6$, $v = 0.379$ (+, − − −); $R_c = 178$, $v = 0.27$ (□, —). Heavy lines are the predictions of the present work, thin lines are those of Hogg (1994) and symbols are experimental results of Jeffrey & Pearson (1965). (*b*) $R_c = 39.2$ (△, — · · —); $R_c = 67.6$ (□, — · —); $R_c = 104.6$ (◇, —); $R_c = 144.4$ (+, − − −). Lines are predictions of the present work and symbols are experimental results of Segré and Silberberg (1962).

be due to the difference in geometry: the experiments were conducted in cylindrical tubes while the calculations were for a plane channel. The second reason is that, for large tube Reynolds numbers the particle Reynolds number, R_p, is not small. So for the experiments performed by Segré & Silberberg (1962*b*) at tube Reynolds numbers 116, 232 and 346 one can estimate R_p as 0.34, 0.68 and 1.00 respectively. This may explain why the trend of the predicted equilibrium positions for neutrally buoyant particles with increasing R_c is not the same as the experimental data.

One more reason for poor agreement of theoretical and experimental results may be indicated for the non-neutrally buoyant particles. We compare in figure 13 (*a*) the lift on a particle divided by the slip velocity, V'. However, the latter was not measured in the experiments. Jeffrey & Pearson (1965) assumed that the slip velocity is equal to the Stokes free-fall velocity, V'_S. The same value is taken in our calculations. Nevertheless, they pointed out that even the axial velocities of the particles, U'_p, hardly can be measured with sufficient accuracy. It would be expected that the difference between the real slip velocity, V' and V'_S was even greater. The wide scatter of experimental data supports this conclusion.

8. Conclusions

The inertial migration of a rigid spherical particle translating parallel to the walls within a channel flow has been considered for large channel Reynolds numbers. Matched asymptotic expansions have been used to solve the Oseen-like equations governing the disturbance flow past neutrally or non-neutrally buoyant particles. Solutions of the outer-flow problem with the scaling based on the mean and local shear rates have been constructed. The problem has been reduced to a fourth-order ordinary differential equation for the Fourier transform of lateral velocity.

Within the framework of the approach based on l_p-scaling the non-dimensional lift on a non-neutrally buoyant sphere is characterized by three dimensionless groups: channel Reynolds number, distance from the wall and slip velocity. The dependence on all parameters has been evaluated numerically using the orthonormalization method.

The scaling based on the local shear rate enables the separation of the effects due to the inertia in the unbounded parabolic flow and the inertial interaction with the walls. The wall effect should be taken into account at distances of the order of $lR_c^{-1/2}$ from the wall. In the near-wall layers the lift is close to values corresponding to the linear shear flow, bounded by a single wall. In the remainder of the channel flow the wall effect is negligible, and the outer flow past a sphere can be treated as an unbounded parabolic flow. In this region the lift depends on only two dimensionless groups characterizing the relative sizes of the uniform, linear and parabolic terms in the undisturbed velocity.

The effect of the curvature of the unperturbed velocity profile is significant, and the lift differs from the values corresponding to a linear shear flow even at large Reynolds numbers. The maximum value of the lift in the unbounded parabolic flow is less than that in the linear shear case while for large magnitudes of the slip velocity the lift in the unbounded parabolic flow is many times greater than the linear-shear predictions.

The inertial migration of a neutrally buoyant particle has been considered for channel flow and linear shear flow bounded by a single wall. For the channel flow the wall effect again emerges in the thin layers near the walls. In the major portion of the flow, where wall-induced inertia is negligible, the lift is significantly less. The behaviour of the lift as a function of curvature is very similar to the non-neutrally buoyant case. The dependences evaluated for different channel Reynolds numbers converge to the limiting dependence, which corresponds to the unbounded parabolic flow. The lift in unbounded flow depends only on the curvature of the undisturbed flow. The lift on a neutrally buoyant sphere in a linear shear flow bounded by a single wall is positive for all distances from the wall, i.e. the particle always migrates outward from the wall.

The lift vanishes on the axis of the channel because of the symmetry of the disturbance flow. There exists at least one more equilibrium position for a negative slip velocity and for a neutrally buoyant particle. The equilibrium position nearest to the wall has been evaluated numerically. For small slip velocity the equilibrium position scaled by l_p is almost the same for different Reynolds numbers. For a neutrally buoyant particle this distance grows with the Reynolds number. At large slip velocities (both negative and positive) additional equilibrium positions arise.

The comparison with the experimental results shows only qualitative agreement for the non-neutrally buoyant particles. The predictions of the lift and equilibrium position for the neutrally buoyant particles agree better with the experimental data.

The research was supported by the International Science and Technology Center (ISTC) under Project No. 199 and the Russian Foundation for Fundamental Research (Grant No. 96-01-01245). The author is grateful for the help in performing of numerical calculations from Sergei Manuilovich. Helpful comments from the Referees were gratefully appreciated.

Appendix

In this Appendix a short overview of the numerical procedure used to calculate $\widetilde{U}_z\left(k_x, k_y, 0\right)$ is given. First we define

$$\boldsymbol{\varphi} = \left(\varphi, \frac{\mathrm{d}\varphi}{\mathrm{d}z}, \frac{\mathrm{d}^2\varphi}{\mathrm{d}z^2}, \frac{\mathrm{d}^3\varphi}{\mathrm{d}z^3}\right).$$

The fourth-order ordinary differential equation has four linearly independent solutions $\boldsymbol{\varphi}_i$, $i = 1$–4. They may be introduced for $Z \leqslant 0$ as

$$\boldsymbol{\varphi}_1^- = (1,0,0,0),\ \boldsymbol{\varphi}_2^- = (0,1,0,0),\ \boldsymbol{\varphi}_3^- = (0,0,1,0),\ \boldsymbol{\varphi}_4^- = (0,0,0,1) \text{ on } Z = -R_c^{1/2} d/l. \tag{A 1}$$

These solutions provide the initial conditions for the numerical integration. Two of them, $\boldsymbol{\varphi}_3^-$ and $\boldsymbol{\varphi}_4^-$, satisfy the boundary conditions (3.9 *b*). Hence an arbitrary solution of (3.9 *a*) for $Z < 0$ satisfying (3.9 *b*) may be sought as

$$\widetilde{U}_z = c_3^- \boldsymbol{\varphi}_3^- + c_4^- \boldsymbol{\varphi}_4^- \quad \text{for} \quad Z \leqslant 0.$$

The initial values for the solutions at $Z \geqslant 0$, $\boldsymbol{\varphi}_i^+$, $i = 1$–4, are introduced on $Z = R_c^{1/2}\left(1 - d/l\right)$ similarly to (A 1). The arbitrary solution satisfying the boundary conditions on the upper wall is

$$\widetilde{U}_z = c_3^+ \boldsymbol{\varphi}_3^+ + c_4^+ \boldsymbol{\varphi}_4^+ \quad \text{for} \quad Z \geqslant 0.$$

Thus, it is necessary to integrate numerically only two solutions. Starting with the above initial conditions, we integrate $\boldsymbol{\varphi}_3^-$, $\boldsymbol{\varphi}_4^-$ upward and $\boldsymbol{\varphi}_3^+$, $\boldsymbol{\varphi}_4^+$ downward to $Z = 0$.

Four unknown constants $c_3^-, c_4^-, c_3^+, c_4^+$ are then determined by the conditions at $Z = 0$. In view of (3.10) they can be written for a non-neutrally buoyant particle as

$$\begin{pmatrix} \varphi_3^- & \mathrm{d}\varphi_3^-/\mathrm{d}Z & \mathrm{d}^2\varphi_3^-/\mathrm{d}Z^2 & \mathrm{d}^3\varphi_3^-/\mathrm{d}Z^3 \\ \varphi_4^- & \mathrm{d}\varphi_4^-/\mathrm{d}Z & \mathrm{d}^2\varphi_4^-/\mathrm{d}Z^2 & \mathrm{d}^3\varphi_4^-/\mathrm{d}Z^3 \\ -\varphi_3^+ & -\mathrm{d}\varphi_3^+/\mathrm{d}Z & -\mathrm{d}^2\varphi_3^+/\mathrm{d}Z^2 & -\mathrm{d}^3\varphi_3^+/\mathrm{d}Z^3 \\ -\varphi_4^+ & -\mathrm{d}\varphi_4^+/\mathrm{d}Z & -\mathrm{d}^2\varphi_4^+/\mathrm{d}Z^2 & -\mathrm{d}^3\varphi_4^+/\mathrm{d}Z^3 \end{pmatrix} \begin{pmatrix} c_3^- \\ c_4^- \\ c_3^+ \\ c_4^+ \end{pmatrix} = \begin{pmatrix} 0 \\ 0 \\ -\mathrm{i}k_x V 3/2\pi \\ 0 \end{pmatrix}. \tag{A 2}$$

One can derive another set of linearly independent solutions of (3.9 *a*) at large k. The second and third terms in brackets in (3.9 *a*) can be neglected when k tends to infinity. As a result one can readily obtain

$$\widehat{\varphi}_1 = \mathrm{e}^{-kZ}, \quad \widehat{\varphi}_2 = Z\mathrm{e}^{-kZ}, \quad \widehat{\varphi}_3 = \mathrm{e}^{kZ}, \quad \widehat{\varphi}_4 = Z\mathrm{e}^{kZ} \quad \text{as} \quad k \to \infty, \quad Z = O(1). \tag{A 3}$$

Two of solutions, $\widehat{\varphi}_1$ and $\widehat{\varphi}_2$, exponentially grow while two others, $\widehat{\varphi}_3$ and $\widehat{\varphi}_4$, exponentially decay at $Z < 0$, and vice versa at $Z > 0$.

One should keep all the linearly independent solutions to find from (A 2) the constants $c_3^-, c_4^-, c_3^+, c_4^+$ with the accuracy required. However, at large R_c this requirement hardly can be fulfilled even for not-too-large k. The reason is that the channel width, when expressed in terms of the lengthscale of the outer region, grows with R_c (see (3.9 *b*)), i.e. the channel boundaries are too far from the particle in this case. The routine numerical technique does not permit the decaying solution to be resolved properly when the path of integration is large. As a result any numerical solution will be the superposition of growing solutions only, whatever its initial value.

This problem is eliminated using the orthonormalization method (Godunov 1961; Conte 1966). When the ratio of magnitudes of different linearly independent solutions becomes large, the Gram–Schmidt orthonormalization procedure is used to construct the new set of linearly independent solutions.

Mack (1976) modified this technique for the case when the problem is unbounded, and the boundary conditions (3.9 *b*) on the wall should be replaced by the vanishing condition for the disturbance flow at infinity. In this case the integration starts at sufficiently large distance where the analytical expressions for the linearly independent solutions can be obtained. A similar approach is used in the present work to evaluate $\Gamma_z\left(q_x, q_y, 0\right)$ for unbounded flow or the flow bounded by a single wall (see §§ 4.1, 6.1).

REFERENCES

Asmolov, E. S. 1989 Lift force exerted on a spherical particle in a laminar boundary layer. *Fluid Dyn.* **24**, 710–714.

Asmolov, E. S. 1990 Dynamics of a spherical particle in a laminar boundary layer. *Fluid Dyn.* **25**, 886–890.

Asmolov, E. S. & Manuilovich, S. V. 1997 Stability of dusty-gas channel flow with non-uniform distribution of particle density. In *3rd European Fluid Mechanics Conference (EUROMECH), Goettingen/Germany, Book of Abstracts*, p. 23.

Asmolov, E. S. & Manuilovich, S. V. 1998 Stability of dusty-gas laminar boundary layer on a flat plate. *J. Fluid Mech.* **365**, 137–170.

Bretherton, F. P. 1962 The motion of rigid particles in a shear flow at low Reynolds number. *J. Fluid Mech.* **24**, 284–304.

Cherukat, P., McLaughlin, J. B. & Graham, A. L. 1994 The inertial lift on a rigid sphere translating in a linear shear flow field. *Intl J. Multiphase Flow* **20**, 339–353.

Conte, S. D. 1966 *SIAM Rev.* **8**, 309.

Cox, R. G. & Brenner, H. 1968 The lateral migration of solid particles in Poiseuille flow. I. Theory. *Chem. Engng Sci.* **23**, 147–173.

Cox, R. G. & Hsu, S. K. 1977 The lateral migration of solid particles in a laminar flow near a plane. *Intl J. Multiphase Flow* **3**, 201–222.

Drew, D. A. 1988 The lift force on a small sphere in the presence of a wall. *Chem. Engng Sci.* **43**, 769–773.

Eichorn, R. & Small, S. 1964 Experiments on the lift and drag of spheres suspended in Poiseuille flow. *J. Fluid Mech.* **20**, 513–527.

Godunov, S. K. 1961 On the numerical solution of the boundary-value problem for the system of linear ordinary differential equations. *Usp. Mat. Nauk* **16,** No. 3, 171–174. (In Russian.)

Ho, B. P. & Leal, L. G. 1974 Inertial migration of rigid spheres in two-dimensional unidirectional flows. *J. Fluid Mech.* **65**, 365–400.

Hogg, A. J. 1994 The inertial migration of non-neutrally buoyant spherical particles in two-dimensional shear flows. *J. Fluid Mech.* **272**, 285–318.

Jeffrey, R. C. & Pearson, J. R. A. 1965 Particle motion in laminar vertical tube flow. *J. Fluid Mech.* **22**, 721–735.

Mack L. M. 1976 A numerical study of the temporal eigenvalue spectrum of the Blasius boundary layer. *J. Fluid Mech.* **73**, 497–520.

McLaughlin, J. B. 1991 Inertial migration of a small sphere in linear shear flows. *J. Fluid Mech.* **224**, 261–274.

McLaughlin, J. B. 1993 The lift on a small sphere in wall-bounded linear shear flows. *J. Fluid Mech.* **246**, 249–265.

Orszag, S. A. 1971 Accurate solution of the Orr-Sommerfeld equation. *J. Fluid Mech.* **50,** 689–703.

Proudman, I. & Pearson, J. R. A. 1957 Expansions at small Reynolds numbers for the flow past a sphere and a circular cylinder. *J. Fluid Mech.* **2**, 237–262.

Saffman, P. G. 1965 The lift on a small sphere in a slow shear flow. *J. Fluid Mech.* **22**, 385–400; and Corrigendum *J. Fluid Mech.* **31**, 1968, 624.

Schonberg, J. A. & Hinch, E. J. 1989 Inertial migration of a sphere in Poiseuille flow. *J. Fluid Mech.* **203**, 517–524.

Segré, G. & Silberberg, A. 1962*a* Behaviour of macroscopic rigid spheres in Poiseuille flow. Part 1. Determination of local concentration by statistical analysis of particle passages through crossed light beams. *J. Fluid Mech.* **14**, 115–135.

Segré, G. & Silberberg, A. 1962*b* Behaviour of macroscopic rigid spheres in Poiseuille flow. Part 2. Experimental results and interpretation. *J. Fluid Mech.* **14**, 136–157.

Shaqfeh, E. S. G. & Acrivos, A. 1987 The effects of inertia on the stability of the convective flow in inclined particle settlers. *Phys. Fluids* **30**, 960–973.

Vasseur, P. & Cox, R. G. 1976 The lateral migration of a spherical particle in two-dimensional shear flows. *J. Fluid Mech.* **78**, 385–413.

Vasseur, P. & Cox, R. G. 1977 The lateral migration of spherical particles sedimenting in a stagnant bounded fluid. *J. Fluid Mech.* **80**, 561–591.